Investigating the dominant corrections to the strong-stretching theory for dry polymeric brushes

M. W. Matsen
Department of Physics, University of Reading, Whiteknights, Reading RG6 6AF, United Kingdom

(Received 15 March 2004; accepted 30 April 2004)

The accuracy of strong-stretching theory (SST) is examined against a detailed comparison to self-consistent field theory (SCFT) on dry polymeric brushes with thicknesses of up to ~17 times the natural chain extension. The comparison provides the strongest evidence to date that SST represents the exact thick-brush limit of SCFT. More importantly, it allows us to assess the effectiveness of proposed finite-stretching corrections to SST. Including the entropy of the free ends is shown to rectify the most severe inaccuracies in SST. The proximal layer proposed by Likhtman and Semenov provides another significant improvement, and we identify one further effect of similar importance for which there is not yet an accurate treatment. Furthermore, our study provides a valuable means of rejecting mistaken refinements to SST, and indeed one such example is revealed. A proper treatment of finite-stretching corrections is vital to a wide range of phenomena that depend on a small excess free energy, such as autophobic dewetting and the interaction between opposing brushes. © *2004 American Institute of Physics.* [DOI: 10.1063/1.1765101]

I. INTRODUCTION

In a seminal 1985 publication, Semenov[1] introduced a strong-stretching theory (SST) to describe block copolymer melts, which was subsequently employed by Milner *et al.*[2] to model polymeric brushes. The theory is based upon the Gaussian chain model for high-molecular weight polymers and treats the molecular interactions using mean-field theory.[3] By assuming each polymer chain is so highly stretched that its *coarse-grained* configuration is restricted to a path of minimum energy, SST is able to provide explicit formulas for a wide range of quantities. The intuitive understanding generated by this simple analytical theory has proven to be invaluable, although it relies on a very stringent assumption. The more general self-consistent field theory (SCFT) (Refs. 4, 5) provides much improved accuracy by considering all possible polymer configurations and weighting each of them by the appropriate Boltzmann factor. However, SCFT is a numerical theory, and thus its predictions cannot be summarized in nice explicit formulas. For this reason, the polymer community continues to embrace both theories, SST for its analytical expressions and SCFT for its improved accuracy.

It is believed that SCFT converges exactly to SST in the limit of strongly-stretched polymers, but this has yet to be confirmed. Indeed, various SST predictions coincide well with SCFT (such as domain sizes in block copolymer melts[6]), but there are also many other quantities for which the comparison is particularly poor. For instance, the SST prediction[7] for the interfacial tension between a polymeric brush and its parent homopolymer is ~5 times that of the SCFT prediction,[8] which incidentally is in good agreement with experiment.[9] More concerning than this quantitative difference is the serious qualitative disagreement regarding the actual source of the tension; SST predicts that it is largely due to changes in the free energy of the brush, while SCFT attributes it almost entirely to the homopolymer. In another instance, where assertive efforts were made to extrapolate SCFT predictions for the phase boundaries of diblock copolymer melts to the SST limit, it appears that the two theories are again inconsistent.[10]

Regardless of whether or not SST represents the proper limit of SCFT, it is certainly clear that the strong-stretching assumption of SST is far from realized at the experimentally relevant conditions, where the SCFT calculations are generally performed. This fact has motivated several attempts to improve upon the standard SST by incorporating finite-stretching corrections.[11–15] Ideally, such studies would provide an improved analytical (or semianalytical) theory, but should provide, at the very least, a deeper understanding for the limitations of SST. However, these efforts have been complicated by the lack of a unique welldefined strategy for incorporating such corrections. Indeed, two of the more significant attempts by Goveas *et al.*[11] and by Likhtman and Semenov[12] involve very distinct approaches and produce vastly different predictions.

Fortunately, SCFT offers a means of testing proposed corrections to SST, and, according to the initial evidence,[16,17] the Likhtman-Semenov approach appears more successful. For a dry brush of thickness L consisting of polymer chains with N segments of statistical length a the improved L-S theory predicts an average free energy per chain,

$$\frac{f}{k_BT}\approx\frac{\pi^2L^2}{8a^2N}-\ln\left(\frac{\sqrt{3}L}{2aN^{1/2}}\right)-K_\xi\left(\frac{L}{aN^{1/2}}\right)^{-2/3}+K_\mu, \quad (1)$$

where $K_\xi\approx 0.374$ and $K_\mu=0.1544$. The first term is the bare SST prediction, the next two terms result from the entropy of the free ends, and the last term comes from a narrow *proximal* layer next to the substrate. SCFT calculations have not yet been performed at sufficient L to directly confirm Eq. (1), but they have corroborated some of the other predictions

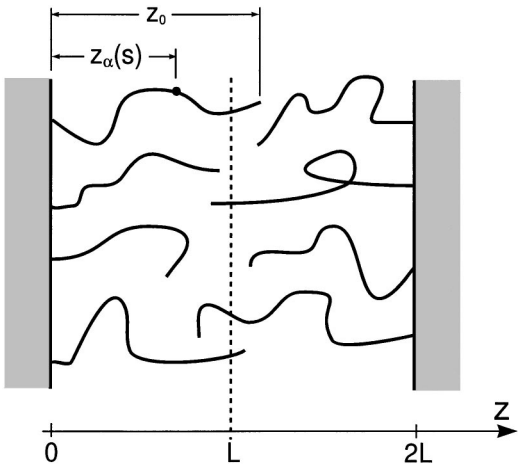

FIG. 1. Schematic diagram of two opposing brushes grafted to substrates at $z=0$ and $2L$ such that they interpenetrate at the $z=L$ midplane denoted by the dashed line. The trajectory, $z_\alpha(s)$, specifies the z coordinate of the sNth segment of the αth polymer. Note that the overall extension of the chain is given by $z_0=z_\alpha(0)$.

regarding significant refinements to the self-consistent field, the distribution of chain ends, and the brush profile.[16,17] If the L-S theory does, indeed, capture the dominant corrections to SST, then it would follow that SCFT→SST in the $L\to\infty$ limit. However, the past comparisons with SCFT are still far from conclusive, and they certainly do not rule out the possible existence of additional corrections that might actually persist into the thick-brush limit.

In this paper, we perform accurate SCFT calculations for brushes with thicknesses of up to $L=8aN^{1/2}$, which represents $\sim$17 times the natural chain extension.[18] A detailed examination of all the relevant quantities provides the first solid evidence that SCFT→SST, at least for the case of flat dry polymeric brushes. Furthermore, we demonstrate that the free energy per chain is consistent with Eq. (1), provided the coefficient K_ξ is adjusted.

II. THEORY

This section provides the theory for a dry polymeric brush of flexible monodisperse chains. The flexibility assumption allows us to treat the substrate and the outer air interface with reflecting boundaries, which in turn implies that a single brush is mathematically equivalent to two opposing brushes.[8] For reasons of convenience, we present the theory in terms of the latter system involving identical brushes grafted to flat parallel substrates at $z=0$ and $z=2L$ as sketched in Fig. 1.

To specify the polymer configurations, each molecule is parametrized along its length, starting from $s=0$ at the free end and running to $s=1$ at the grafted end. With that, the configuration of the αth polymer can be expressed as $\mathbf{r}_\alpha(s)$. However, for the special planar geometry consider here, we need only be concerned with the z component of the trajectory, $z_\alpha(s)$. The motion in the x-y plane is completely decoupled, and obeys simple random-walk statistics.[8]

In the z direction, the chains must deviate from a random walk in order to avoid an overcrowding of segments near the substrate. Rather than explicitly including the hard-core interactions responsible for this, a Lagrange-multiplier field $w(z)$ is introduced to enforce a uniform polymer concentration by penalizing segments close to the substrate. With that, the energy E for a portion of the chain ($s_1\leqslant s\leqslant s_2$) is given by

$$\frac{E[z_\alpha;s_1,s_2]}{k_BT}=\int_{s_1}^{s_2}\left(\frac{3[z'_\alpha(s)]^2}{2a^2N}+w(z_\alpha(s))\right)ds, \tag{2}$$

where the first term represents the entropic penalty of stretching the polymer and the second term is the energy due to the field.[4]

A. Self-consistent field theory

At the heart of SCFT is the partition function $q(z,z_0,s)$ for a fragment of chain with sN segments extending between z and z_0. It is given by the functional integral,

$$q(z,z_0,s)\propto\int\mathcal{D}z_\alpha\exp\left(-\frac{E[z_\alpha;0,s]}{k_BT}\right)\times\delta(z_\alpha(0)-z_0)\delta(z_\alpha(s)-z), \tag{3}$$

which can be evaluated by solving[4,5]

$$\frac{\partial}{\partial s}q(z,z_0,s)=\frac{a^2N}{6}\frac{\partial^2}{\partial z^2}q(z,z_0,s)-w(z)q(z,z_0,s), \tag{4}$$

subject to reflecting boundary conditions at $z=0$ and $z=2L$ and an initial condition $q(z,z_0,0)=\delta(z-z_0)aN^{1/2}$. Note that in the limit $z_0\to0$, the δ function merges with its reflection giving, in that case, an initial condition of $q(z,0,0)=2\delta(z)aN^{1/2}$.

Once $q(z,z_0,s)$ is known, the free energy of a complete chain extended from the $z=0$ substrate to $z=z_0$ is given by

$$\frac{f_0(z_0)}{k_BT}=-\ln q(0,z_0,1)+\ln\sqrt{3}-\frac{1}{4}. \tag{5}$$

Since the definition in Eq. (3) does not specify an absolute magnitude for $q(z,z_0,s)$, $f_0(z_0)$ is only defined within an additive constant. In Eq. (5), we choose a particular constant for reasons that will become apparent in Sec. II D. Given $f_0(z_0)$, the distribution of chain ends is specified by the Boltzmann weight,

$$g(z_0)=\frac{aN^{1/2}}{\mathcal{Q}}\exp\left(-\frac{f_0(z_0)}{k_BT}\right), \tag{6}$$

where

$$\mathcal{Q}=\int_0^{2L}\exp\left(-\frac{f_0(z_0)}{k_BT}\right)dz_0 \tag{7}$$

is the partition function for a single chain with one end free and the other end attached to the $z=0$ substrate.

The next step is to evaluate the concentration profile $\phi(z)$ of the brush grafted to the $z=0$ substrate. We start with

$$\rho(z;z_0,s)=\frac{q(z,z_0,s)q(0,z,1-s)}{q(0,z_0,1)}, \tag{8}$$

which is the distribution of the sNth segment from a chain extended to $z=z_0$. From this, the segment profile of the entire chain is

$$\phi(z;z_0)=\int_0^1 \rho(z;z_0,s)ds, \tag{9}$$

which in turn gives

$$\phi(z)=\frac{L}{a^2N}\int_0^{2L} g(z_0)\phi(z;z_0)dz_0. \tag{10}$$

Of course, the brush attached to the $z=2L$ substrate has a symmetrical distribution, and their combination must satisfy the incompressibility condition,

$$\phi(z)+\phi(2L-z)=1, \tag{11}$$

which is the criterion used to determine $w(z)$.

Once $w(z)$ is evaluated self-consistently, it is straightforward to compute the average free energy per chain f. First of all, the elastic energy of an individual chain, $f_{0,e}(z_0)=f_0(z_0)-f_{0,w}(z_0)$, extended to $z=z_0$ is obtained by taking $f_0(z_0)$ and subtracting off the fictitious energy of the field,

$$f_{0,w}(z_0)=\frac{k_BT}{aN^{1/2}}\int w(z)\phi(z;z_0)dz. \tag{12}$$

Averaging $f_{0,e}(z_0)$ over the distribution of chain extensions gives the average stretching energy per chain as

$$f_e=\frac{1}{aN^{1/2}}\int g(z_0)f_{0,e}(z_0)dz_0. \tag{13}$$

Second of all, the entropic energy associated with the distribution of the end segments is given by

$$f_g=\frac{k_BT}{aN^{1/2}}\int g(z_0)\ln g(z_0)dz_0. \tag{14}$$

The total free energy is then just the sum, $f=f_e+f_g$.

B. Full classical theory

Here we describe an intermediate theory to SCFT and SST, which we refer to as the full classical theory (FCT).[16] It is similar to SST in that it assumes the chains are so strongly stretched that the partition function in Eq. (3) is completely dominated by the lowest energy path, referred to as the *classical* trajectory because of an analogy with classical mechanics.[2,19] The classical path is obtained by minimizing the integral for $E[z_\alpha;0,1]$ with respect to $z_\alpha(s)$, which is a standard variational calculus problem corresponding to the Euler-Lagrange equation,

$$\frac{d}{ds}\left(\frac{\mathcal{D}E}{\mathcal{D}z'_\alpha}\right)-\left(\frac{\mathcal{D}E}{\mathcal{D}z_\alpha}\right)=0. \tag{15}$$

The functional differentiation of Eq. (2) gives the second-order differential equation,

$$\frac{d}{ds}\left(\frac{3z'_\alpha(s)}{a^2N}\right)-w'(z_\alpha(s))=0. \tag{16}$$

Rearranging this as

$$\frac{d}{ds}\left(\frac{3[z'_\alpha(s)]^2}{2a^2N}\right)-\frac{d}{ds}w(z_\alpha(s))=0, \tag{17}$$

allows us to perform one integration, reducing it to the first-order equation,

$$\frac{3[z'_\alpha(s)]^2}{2a^2N}-w(z_\alpha(s))=\frac{3v_0^2}{2a^2N}-w(z_0), \tag{18}$$

where the constant of integration has been expressed in terms of the initial conditions, $z_0\equiv z_\alpha(0)$ and $v_0\equiv -z'_\alpha(0)$. The parameter v_0 has to be adjusted so that $z_\alpha(1)=0$.

Once the classical path $z_\alpha(s)$ is determined, the free energy is treated with the ground-state approximation,

$$f_0(z_0)=E[z_\alpha;0,1], \tag{19}$$

and segment distributions are taken to be

$$\rho(z;z_0,s)=\delta(z-z_\alpha(s))aN^{1/2}. \tag{20}$$

From there on, the FCT proceeds exactly as SCFT.

C. Strong-stretching theory

In the FCT, a small population of chains extend beyond the midplane, because the extra stretching penalty is compensated for by the entropic advantage of having a wider end-segment distribution, $g(z_0)$. However, this advantage diminishes as $L\to\infty$, and the FCT reduces to the conventional SST, where there is no interpenetration between the brushes, in which case we need only consider $z<L$. As the effect of the end-segment entropy vanishes, so does the tension at the free end of the chain (i.e., $v_0\to 0$), from which a classical-mechanics analogy[19] with a simple harmonic oscillator leads us to conclude that

$$w(z)=-\frac{3\pi^2z^2}{8a^2N}. \tag{21}$$

Indeed, the corresponding trajectory,

$$z_\alpha(s)=z_0\cos(\pi s/2), \tag{22}$$

has a derivative of zero at $s=0$. However, at this level of approximation, $f_0(z_0)=E[z_\alpha;0,1]=0$ and therefore $g(z_0)$ must be obtained by another means other than Eq. (6).

Inserting the above trajectory into Eq. (20), and integrating $\rho(z;z_0,s)$ over s gives

$$\phi(z;z_0)=\begin{cases}\dfrac{2aN^{1/2}}{\pi\sqrt{z_0^2-z^2}}, & \text{if } z<z_0\\ 0, & \text{if } z>z_0.\end{cases} \tag{23}$$

Since the brushes no longer interpenetrate, it follows that $\phi(z)=1$ for $z<L$. Therefore, Eq. (10) can be inverted to obtain

$$g(z_0)=\frac{z_0aN^{1/2}}{L\sqrt{L^2-z_0^2}}, \tag{24}$$

for $z_0<L$.

A straightforward calculation gives the stretching energy of an individual chain as

$$\frac{f_{0,e}(z_0)}{k_BT}=\frac{3\pi^2 z_0^2}{16a^2N}. \tag{25}$$

Weighting this with respect to $g(z_0)$ gives an average stretching energy per chain of

$$\frac{f_e}{k_BT}=\frac{\pi^2L^2}{8a^2N}. \tag{26}$$

In the SST limit, $f_e \gg f_g$, and thus the free energy per chain is approximated as $f \approx f_e$ [i.e., the first term in Eq. (1)].

D. SCFT for the parabolic potential

Normally, the partition function in SCFT has to be evaluated numerically, but it can be solved exactly[20] for the SST potential in Eq. (21). In this case, the solution to Eq. (4) is

$$q(z,z_0,s) = \left(\frac{3}{\sin(\pi s/2)}\right)^{1/2} \exp\left(-\frac{3\pi(z^2+z_0^2)}{4a^2N\tan(\pi s/2)}\right) \times \cosh\left(\frac{3\pi z z_0}{2a^2N\sin(\pi s/2)}\right), \tag{27}$$

where we only enforce the reflecting boundary at $z=0$. From this, it immediately follows that

$$\frac{f_0(z_0)}{k_BT}=-\frac{1}{4} \tag{28}$$

and

$$\rho(z;z_0,s)=\left(\frac{3}{2\sin(\pi s)}\right)^{1/2} \times\left[\exp\left(-\frac{3\pi[z-z_0\cos(\pi s/2)]^2}{2a^2N\sin(\pi s)}\right) +\exp\left(-\frac{3\pi[z+z_0\cos(\pi s/2)]^2}{2a^2N\sin(\pi s)}\right)\right]. \tag{29}$$

Note that the second exponential, due to the reflecting boundary, can generally be ignored provided s is not too close to one. Although there is no analytic formula for $\phi(z;z_0)$, we can still obtain one for

$$\frac{f_{0,w}(z_0)}{k_BT}=\int w(z)\rho(z;z_0,s)\,dz\,ds=-\frac{3\pi^2z_0^2}{16a^2N}-\frac{1}{4} \tag{30}$$

by integrating first over z and then s. Note that the stretching energy, $f_{0,e}(z_0)=f_0(z_0)-f_{0,w}(z_0)$, exactly matches the SST prediction in Eq. (25); it was this that motivated our choice for the additive constant in Eq. (5).

E. Numerical algorithm for SCFT

In previous work,[8] we solved the SCFT using a spectral (i.e., Fourier) method, but it was unable to cope with $L \gtrsim 2aN^{1/2}$. This is due to an inability to represent the initial condition, $q(z,z_0,0)=0$ for $z\neq z_0$, with sufficient accuracy. When the brush is very thick, the strong negative field at $z \approx L$ amplifies the numerical noise, which eventually overwhelms the solution. The noise grows exponentially, and consequently it is futile to combat the problem by increasing the number of Fourier terms. This particular problem would also plague semispectral methods.[21]

Thus we are obliged to solve the SCFT using a real-space algorithm. Concerned with the presence of δ functions in the field $w(z)$ and the initial condition $q(z,z_0,0)$ we explored a number of sophisticated approaches but eventually concluded that it is best to apply a simple method using a very fine mesh. We start by defining $q_{i,j}\equiv q(i\Delta z,z_0,j\Delta s)$ and $w_i\equiv w(i\Delta z)$, where $\Delta z=L/M$ and $\Delta s=1/N$. The diffusion equation is then approximated as

$$\frac{q_{i,j+1}-q_{i,j}}{\Delta s}=\frac{a^2N}{12(\Delta z)^2}(q_{i+1,j+1}-2q_{i,j+1}+q_{i-1,j+1} +q_{i+1,j}-2q_{i,j}+q_{i-1,j}) +\frac{w_i}{2}(q_{i,j+1}+q_{i,j}), \tag{31}$$

which corresponds to the well-known Crank-Nicolson procedure.[22] The reflecting boundaries are treated by setting $q_{-1,j}=q_{1,j}$ and $q_{2M+1,j}=q_{2M-1,j}$, and then the resulting set of linear algebraic equations is solved iteratively starting with the known solution for $j=0$ and stepping through to $j=N$.

The diffusion equation (4) has the property that it conserves the concentration of segments [i.e., the integral of $\phi(z)$ is fixed regardless of $w(z)$], but small violations can occur with the discrete version in Eq. (31). This has dire consequences when attempting to solve $w(z)$ for thick brushes. Fortunately, the conservation of segments is restored if all the integrals are performed using the simple trapezoid method,[22]

$$\int_0^{2L} f(z)dz \approx \left(\frac{f(0)}{2}+\sum_{i=1}^{2M-1} f(i\Delta z)+\frac{f(2L)}{2}\right)\Delta z, \tag{32}$$

where $f(z)$ is an arbitrary integrand.

Naturally, the discrete representation in Eq. (31) will be accurate when $q(z,z_0,s)$ and $w(z)$ vary slowly with respect to the mesh size, but it is impossible to choose Δz sufficiently small to satisfy this condition everywhere because of the δ functions involved. Fortunately again, the Crank-Nicolson method remains accurate provided the Dirac δ functions are replaced with Kronecker δ functions according to

$$\delta(z-z_0)\rightarrow \delta_{i,j}/\Delta z, \tag{33}$$

where $z=i\Delta z$ and $z_0=j\Delta z$. We have confirmed this by testing against the analytical solutions for a parabolic potential [in Eq. (27)], and for $w(z)\propto\delta(z)$ [in Ref. 12]. We have also

used these known solutions to gauge the necessary number of mesh points. For our required accuracy, $M=10\,000$ and $N=20\,000$ are sufficient.

The most computational aspect of SCFT is the determination of $w(z)$. There are a few things we do to maximize the efficiency of this procedure. First of all, we solve Eq. (31) with reflecting boundaries at $z=0$ and $z=L$, once for $q(z,s)\equiv q(z,0,s)$ with initial condition $q(z,0)=2\delta(z)aN^{1/2}$, and again for $q^{\dagger}(z,s)\equiv\int q(z,z_0,s)dz_0/aN^{1/2}$ with $q^{\dagger}(z;0)=1$. The total segment concentration of the two opposing brushes is then evaluated using

$$\phi(z)+\phi(2L-z)=\frac{L}{q^{\dagger}(0,1)aN^{1/2}}\int_0^1 q(z,1-s)q^{\dagger}(z,s)ds. \tag{34}$$

We start with an accurate estimate of $w(z)$ obtained from the FCT prediction corrected for the proximal layer. This initial guess is then improved upon with a Picard iteration scheme, where $\lambda[\phi(z)+\phi(2L-z)-1]$ is repeatedly added to $w(z)$ (with $\lambda\approx 0.1$) until $|\phi(z)+\phi(2L-z)-1|<10^{-3}$ for all $0\leqslant z\leqslant L$. Finally, we switch to a quasi-Newton scheme (the Broyden method[22]) to obtain an ultra precise solution, where $|\phi(z)+\phi(2L-z)-1|<10^{-9}$.

III. RESULTS

This section begins with a detailed comparison between SCFT, FCT, and SST. The aim is twofold. The first is to demonstrate that FCT provides a substantial improvement over SST, and the second is to provide clear evidence that SCFT converges to the FCT in the thick-brush limit. Once this is established, we finish by investigating the effects of fluctuations about the classical path, responsible for the remaining differences between SCFT and FCT.

Figure 2(a) compares the self-consistent fields $w(z)$ predicted by SCFT, FCT, and SST at $L=4aN^{1/2}$. The comparison involves a slight ambiguity because the theories are unaffected by an additive constant to $w(z)$. The FCT and SST fields are typically chosen with $w(0)=0$, but this is impossible in SCFT because of a δ function at $z=0$. So we, instead, shift the SCFT curve so that it matches the FCT one at $z\approx 0.6L$. This provides the best agreement between SCFT and FCT, much better than what can be achieved between SCFT and SST. Figure 2(b) plots the resulting difference $\Delta w(z)$ between the SCFT and FCT predictions over a range of brush thicknesses. By $L=8aN^{1/2}$, the relative difference is minute, with the exception of a narrowing region next to the substrate. As we will soon show, the proximal-layer correction of Likhtman and Semenov[12] accurately accounts for this nonzero $\Delta w(z)$ next to the substrate.

Now we investigate the elastic energy $f_{0,e}(z_0)$ of extending a chain to $z=z_0$. The SCFT, FCT, and SST predictions are plotted in Fig. 3(a) for a brush of $L=4aN^{1/2}$. This time the comparison is absolute, and we can see that the FCT provides a small but distinct improvement over the SST. The difference, $\Delta f_{0,e}(z_0)$, between SCFT and FCT is shown in Fig. 3(b) for brushes of different thickness. The plot provides overwhelming evidence that the relative size of $\Delta f_{0,e}(z_0)$ vanishes as $L\to\infty$.

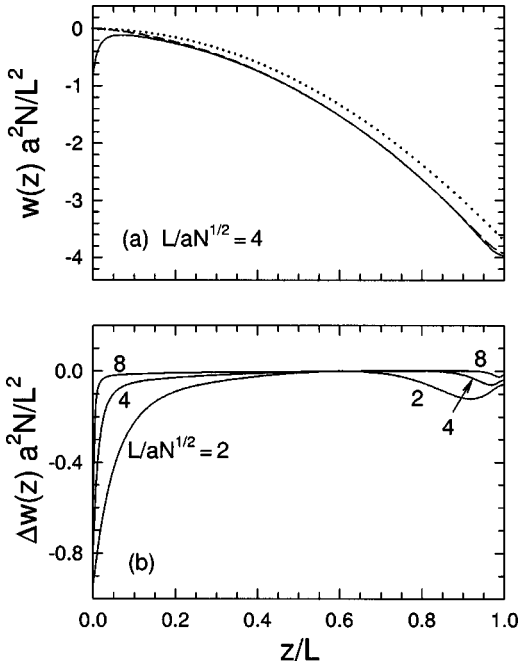

FIG. 2. (a) Self-consistent field $w(z)$ calculated by SCFT (solid), FCT (dashed), and SST (dotted) for a brush of thickness, $L/aN^{1/2}=4$. (b) The difference $\Delta w(z)$ between the SCFT and FCT predictions plotted for three different brush thicknesses.

The improved prediction for the end-segment distribution function $g(z_0)$ is one of the main achievements[14] of the FCT over SST as demonstrated again in Fig. 4(a). The small remaining difference $\Delta g(z_0)$ between SCFT and FCT plotted in Fig. 4(b) occurs largely because FCT predicts the peak in $g(z_0)$ at slightly larger z_0. Nevertheless, the separation

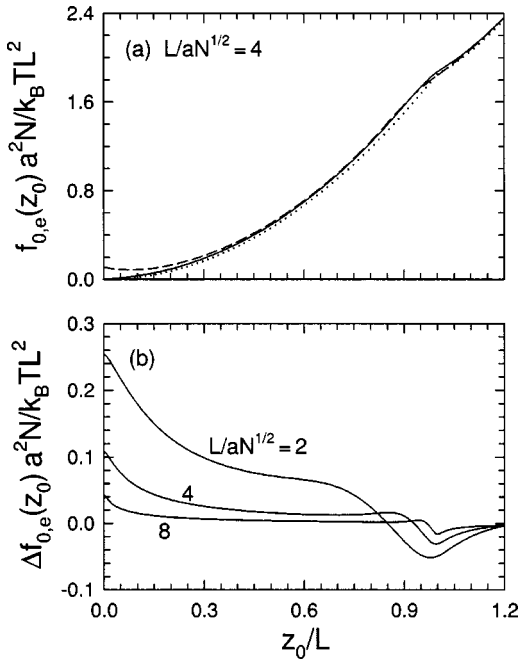

FIG. 3. (a) Elastic energy $f_{0,e}(z_0)$ of a single chain as a function of extension z_0 calculated by SCFT (solid), FCT (dashed), and SST (dotted) for a brush of thickness, $L/aN^{1/2}=4$. (b) The difference $\Delta f_{0,e}(z_0)$ between the SCFT and FCT predictions plotted for three different brush thicknesses.

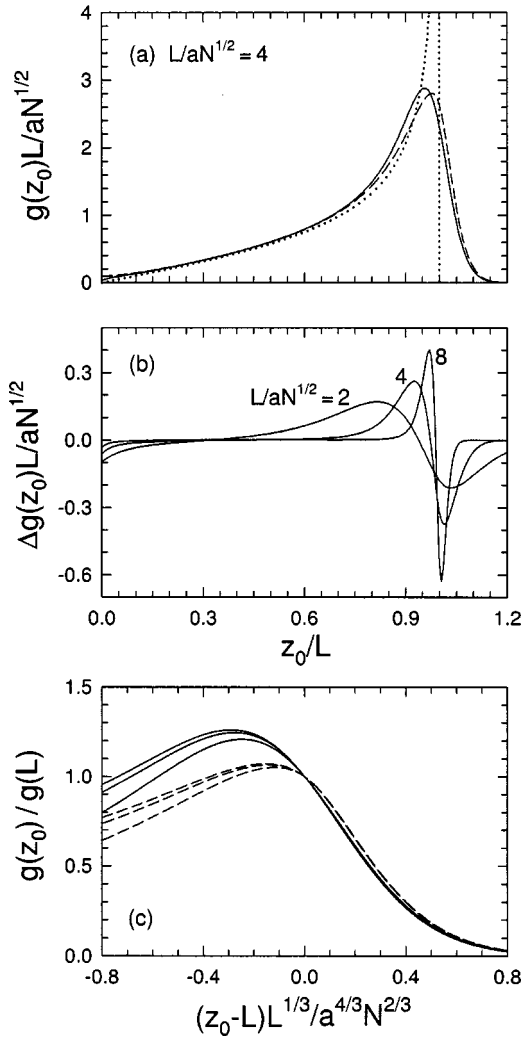

FIG. 4. (a) End-segment distribution $g(z_0)$ calculated by SCFT (solid), FCT (dashed), and SST (dotted) for a brush of thickness, $L/aN^{1/2}=4$. (b) The difference $\Delta g(z_0)$ between the SCFT and FCT predictions plotted for three different brush thicknesses. (c) Scaling plot showing that the tail of $g(z_0)$ for $z_0>L$ scales as $L^{-1/3}$.

between the SCFT and FCT peaks decreases as $L\to\infty$, and thus the two predictions converge. In a previous publication,[16] we showed that FCT predicts the tail of $g(z_0)$ extending beyond $z_0=L$ to scale as $L^{-1/3}$; the scaling plot in Fig. 4(c) now demonstrates that the same is true in SCFT.

The main shortcoming of the FCT is its inability to significantly improve upon the SST estimate for $\phi(z;z_0)$. For all z_0 prior to the peak in $g(z_0)$, the chain trajectories have a turning point where $z'_\alpha(s)=0$. This causes a divergence in $\phi(z;z_0)$ that is not present in SCFT, and consequently our previous comparison between the SCFT and FCT predictions of $\phi(z;z_0)$ at $L=2aN^{1/2}$ was rather poor.[16] This comparison is repeated in Fig. 5 for $L=8aN^{1/2}$, and while the agreement is much better, it is still far from impressive. However, we will soon demonstrate how this difference can be fully accounted for, allowing us to conclude once again that the SCFT and FCT predictions converge as $L\to\infty$.

Figure 6(a) compares the overall segment profile $\phi(z)$ predicted by SCFT and FCT for brushes of various thickness. The FCT consistently predicts a sharper profile, but nevertheless the difference diminishes as $L\to\infty$. We previously demonstrated[16] that the width of the FCT profile scales as $L^{-1/3}$, and Fig. 6(b) now illustrates that the same is true in SCFT. Hence, the SCFT and FCT profiles both converge to the same step function predicted by SST, where there is no interpenetration between the opposing brushes.

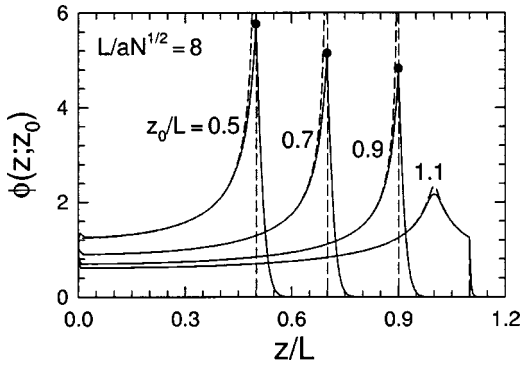

FIG. 5. Segment distribution $\phi(z;z_0)$ of a single chain extended to various z_0 as calculated by SCFT (solid) and FCT (dashed) in a brush of thickness, $L=8aN^{1/2}$. When $g'(z_0)>0$ the FCT predictions diverge whereas the SCFT curves have finite peaks denoted by the solid dots.

Finally, we come to the average free energy per chain f plotted in Fig. 7(a) as a function of brush thickness L. The FCT, which predicts[16]

$$\frac{f}{k_BT}\approx\frac{\pi^2L^2}{8a^2N}-\ln\left(\frac{L}{2aN^{1/2}}\right)-0.84\left(\frac{L}{aN^{1/2}}\right)^{-2/3}, \qquad (35)$$

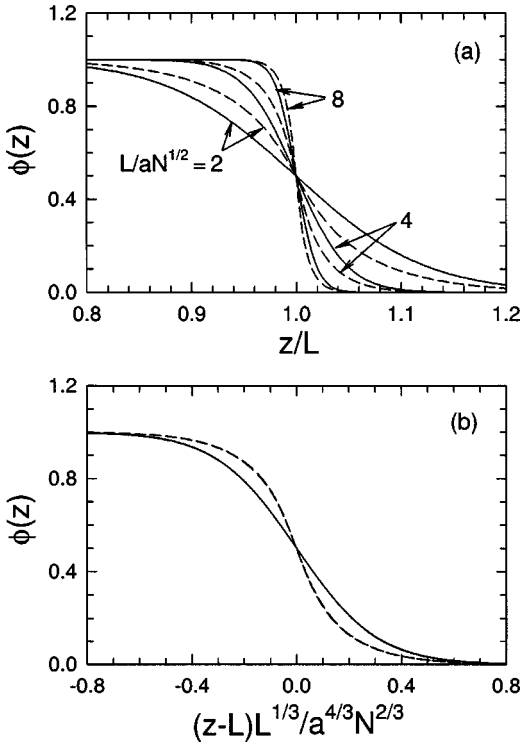

FIG. 6. (a) Brush profile $\phi(z)$ calculated by SCFT (solid) and FCT (dashed) for three different brush thicknesses. (b) Same results replotted in terms of a scaling variable.

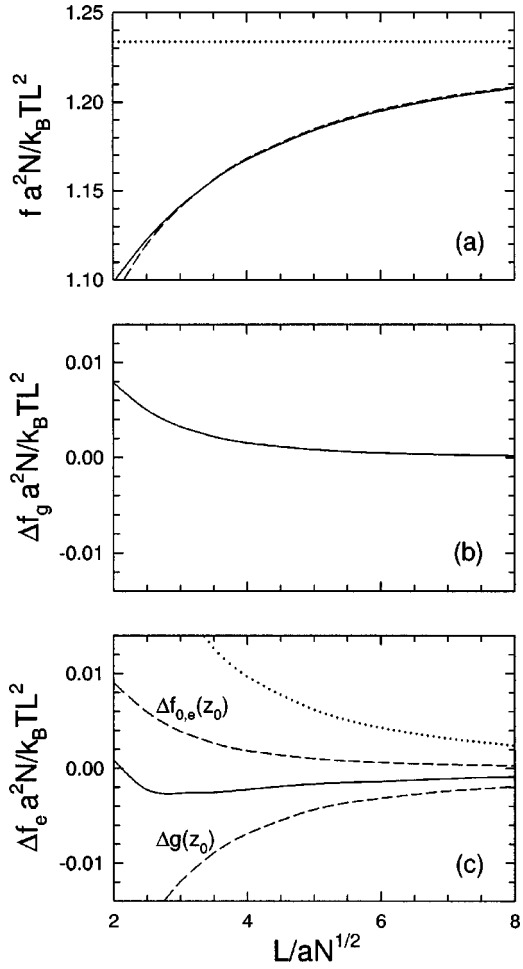

FIG. 7. (a) Average free energy per chain f as a function of brush thickness L calculated by SCFT (solid), FCT (dashed), and SST (dotted). (b) The difference Δf_g between the SCFT and FCT predictions for the entropic free energy associated with the $g(z_0)$ distribution. (c) The difference Δf_e between the SCFT and FCT predictions for the stretching energy. The dashed curves show the approximate contribution due to $\Delta g(z_0)$ and $\Delta f_{0,e}(z_0)$ from Eq. (37), and the dotted curve shows the proximal-layer correction of $0.1544 k_B T$.

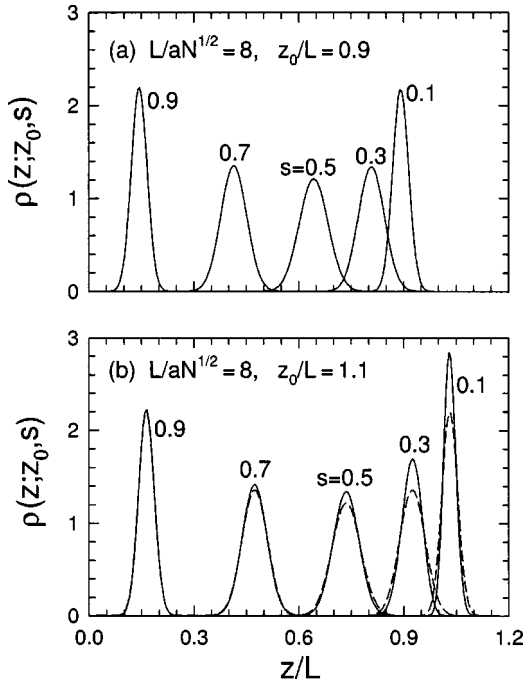

FIG. 8. Profiles, $\rho(z;z_0,s)$, of individual segments calculated with SCFT for chains extended to (a) $z_0/L=0.9$ and (b) $z_0/L=1.1$ in a brush of thickness, $L/aN^{1/2}=8$. The dashed curves denote the Gaussian distributions given by Eq. (38).

provides a remarkable improvement over the SST, which just predicts the first term in Eq. (35). To investigate the difference between the SCFT and FCT, we decompose the free energy as $f=f_g+f_e$. Figure 7(b) shows the difference for f_g, which is well approximated by

$$\Delta f_g \approx \frac{k_B T}{aN^{1/2}} \int \Delta g(z_0)[\ln g(z_0)+1]dz_0. \tag{36}$$

In this case, the inaccuracy Δf_g clearly vanishes relative to f, as it must given that $\Delta g(z_0)$ vanishes relative to $g(z_0)$. Figure 7(c) plots the difference in f_e, which can be conveniently separated as

$$\Delta f_e \approx \frac{1}{aN^{1/2}} \int \Delta g(z_0) f_{0,e}(z_0) dz_0 + \frac{1}{aN^{1/2}} \int g(z_0) \Delta f_{0,e}(z_0) dz_0. \tag{37}$$

The lower and upper dashed curves in Fig. 7(c) show the contributions due to inaccuracies in $g(z_0)$ and $f_{0,e}(z_0)$, respectively. In both cases, the curves show a clear trend towards zero; of course, we should have expected this given our previous evidence that the relative sizes of $\Delta g(z_0)$ and $\Delta f_{0,e}(z_0)$ both vanish as $L\to\infty$. Thus, the convergence of SCFT to FCT appears complete in every respect.

All the corrections beyond the FCT involve fluctuations about the classical trajectory $z_\alpha(s)$. The immediate consequence of these fluctuations is to provide the individual segment distributions $\rho(z;z_0,s)$ with a finite width contrary to the FCT prediction in Eq. (20). Figure 8 illustrates that the SCFT distributions are, in fact, still broad even for brushes of $L=8aN^{1/2}$. Nevertheless, we can rationalize an impressive approximation for these distributions. From our previous work,[26] we know that the peak in $\rho(z;z_0,s)$ is very well approximated by the classical trajectory. If we combine this observation with the Gaussian distributions predicted in Eq. (29) for a parabolic potential, we might expect that

$$\rho(z;z_0,s) \approx \left(\frac{3}{2\sin(\pi s)}\right)^{1/2} \left[\exp\left(-\frac{3\pi[z-z_\alpha(s)]^2}{2a^2 N \sin(\pi s)} \right) + \exp\left(-\frac{3\pi[z+z_\alpha(s)]^2}{2a^2 N \sin(\pi s)} \right) \right]. \tag{38}$$

In fact, this approximation is so good that it is indistinguishable from the SCFT prediction on the scale of Fig. 8(a). Only when the chains are stretched beyond the midplane, as in Fig. 8(b), does the difference become noticeable, but still the agreement remains reasonable.

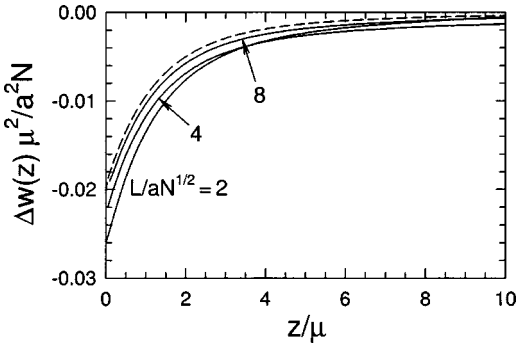

FIG. 9. Results of Fig. 2(b) scaled with respect to the width μ of the proximal layer. The dashed curve denotes $w_r(z/\mu)$ from the proximal-layer correction in Eq. (39).

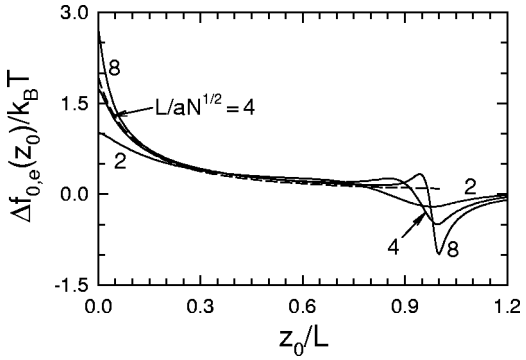

FIG. 10. Results of Fig. 3(b) rescaled and compared with the proximal-layer correction denoted by the dashed curve.

If we integrate Eq. (38) with respect to s, we obtain an excellent approximation for $\phi(z;z_0)$ that is generally indistinguishable from the SCFT predictions in Fig. 5. Again, visible differences do emerge when $z_0 \gtrsim L$, but these remain relatively small. The main exception to the agreement occurs in a very narrow region next to the substrate. The second exponential in Eq. (38), due to the reflecting boundary at $z=0$, causes an excess concentration of segments next to the substrate.

Likhtman and Semenov[12] realized that this excess of segments requires an extra contribution to the field $w(z)$ given by

$$\Delta w(z) \approx \frac{\beta a^2 N}{3}\,\delta(z) + w_r(z/\mu), \tag{39}$$

where $\mu=(2\beta)^{-1}$ is the approximate distance from the substrate over which the field must be modified. The strength of the δ function is given by an average, $\beta=\langle \tau^{-1}\rangle^{-1}$, involving the distribution of chain tensions, $\tau \equiv -3z'_\alpha(1)/a^2N$, at the substrate. Using the distribution predicted by SST, $\beta=3L/a^2N$. Indeed, our SCFT calculations produce a δ function at $z=0$ that agrees with this prediction to within a fraction of a percent over the entire range examined in this paper (i.e., $2aN^{1/2} \leqslant L \leqslant 8aN^{1/2}$). Furthermore, the difference between the SCFT and FCT predictions at finite z agrees well with $w_r(z/\mu)$ as illustrated in Fig. 9.

The proximal layer at $z \lesssim \mu$ causes a significant increase in the stretching energy, particularly for weakly stretched chains. Its effect, shown in Fig. 10, accounts well for the difference $\Delta f_{0,e}(z_0)$ between SCFT and FCT until $z_0 \approx L$. Averaging the proximal-layer correction for $\Delta f_{0,e}(z_0)$ over the SST prediction for $g(z_0)$ gives a contribution to the average stretching energy of $\Delta f_e = 0.1544 k_B T$, which is denoted in Fig. 7(c) by a dotted curve. This somewhat overestimates the upper dashed curve associated with the $\Delta f_{0,e}(z_0)$ contribution in Eq. (37), signifying that we still need to improve our treatment of the strongly stretched chains (i.e., $z_0 \gtrsim L$).

There is one further prediction that verifies the validity of the proximal-layer correction. The FCT predicts that $\phi(z;z_0)$ in Fig. 5 is approximately constant next to the substrate, whereas SCFT predicts the nontrivial profiles shown in the expanded view of Fig. 11 (solid curves). The proximal-layer predictions (dashed curves) are so similar to the SCFT curves as to be visibly indistinguishable for $z_0/L \gtrsim 0.7$.

Just as the broadening of $\rho(z;z_0,s)$ pushes segments toward the substrate, it also causes a build up of segments at the midplane. We demonstrate this by calculating $\phi(z)$ using Eq. (38) with the classical trajectory $z_\alpha(s)$ from the FCT. This is plotted in Fig. 12 along with the combined concentration $\phi(z)+\phi(2L-z)$ of two opposing brushes. As expected, there is approximately a 20% excess of segments at $z \approx L$, which requires another correction akin to the proximal-layer one. The L-S theory also corrects for this build up of segments, but not accurately. Although the development of an accurate treatment is beyond the scope of this paper, we do suggest in the following section how this might be accomplished.

Nevertheless, Semenov[23] claims that an accurate treatment would only increase K_ξ without altering the functional form of Eq. (1). Furthermore, he expects that the next order correction should scale as $L^{-4/3}$. On this basis, we fit our SCFT prediction for the free energy per chain to

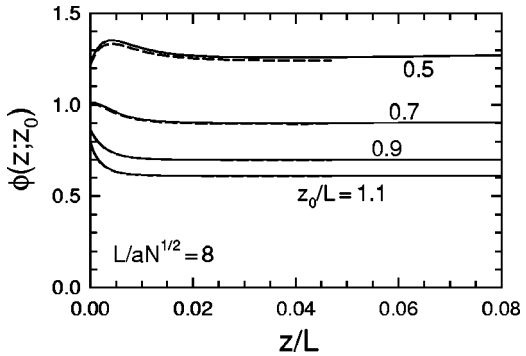

FIG. 11. Magnification of the SCFT profiles in Fig. 5 next to the substrate. The dashed curves show the predictions resulting from the proximal-layer correction.

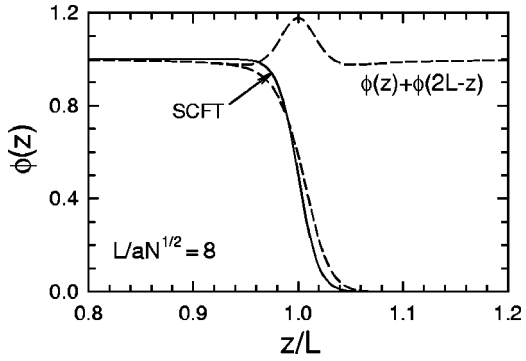

FIG. 12. Brush profile predicted by SCFT (solid) compared to that (dashed) obtained from FCT where $\rho(z;z_0,s)$ is given the finite Gaussian distributions in Eq. (38).

$$\frac{f}{k_BT}\approx\frac{\pi^2L^2}{8a^2N}-\ln\left(\frac{\sqrt{3}L}{2aN^{1/2}}\right)-0.64\left(\frac{L}{aN^{1/2}}\right)^{-2/3}-0.09\left(\frac{L}{aN^{1/2}}\right)^{-4/3}+0.1544. \tag{40}$$

Figure 13 demonstrates that this is, in fact, a truly excellent fit that performs well even down to brush thicknesses characteristic of experiment; this was one of the ultimate goals for considering the finite-stretching corrections to SST.

IV. DISCUSSION

Our detailed comparisons provide conclusive evidence that SCFT converges to FCT in the thick-brush limit. The field $w(z)$, the stretching energy of individual chains $f_{0,e}(z_0)$, the end-segment distribution function $g(z_0)$, and the average free energy per chain f of SCFT all show clear convergence to the FCT predictions. By this, we imply that the relative differences vanish [e.g., $\Delta w(z)/w(z)\to 0$] as $L\to\infty$. It was less obvious that the SCFT prediction for the segment distribution of individual chains $\phi(z;z_0)$ converges to that of FCT, until we demonstrated that the difference is accurately accounted for by the improved approximation of $\rho(z;z_0,s)$ in Eq. (38). Coupling all these facts with our previous demonstration[16] that FCT→SST, we can now confidently conclude that SST represents the correct asymptotic limit of SCFT.

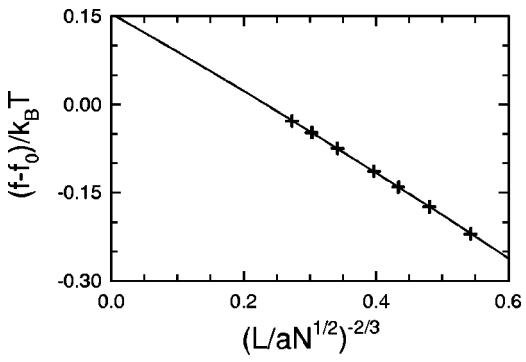

FIG. 13. Difference between the free energy per chain f and the first two terms of Eq. (1), $f_0/k_BT\equiv\pi^2L^2/8a^2N-\ln(\sqrt{3}L/2aN^{1/2})$. In this instance, the added constant, $\ln\sqrt{3}-0.25$, in Eq. (5) has been dropped from f. Crosses denote the actual SCFT calculations, while the solid curve shows the fit given by Eq. (40).

For practical purposes, the entropy of the free chain ends (i.e., $s=0$) and its effect on the end-segment distribution function $g(z_0)$ provides the most substantial correction to SST. This suggests that an effective strategy for incorporating finite-stretching corrections should begin with the FCT, before accounting for fluctuations about the classical paths. Unfortunately, Goveas *et al.*[11] chose instead to expand about the classical paths of SST in Eq. (22). In their systematic expansion, analogous to the WKB approximation in quantum mechanics, the first-order correction produced no improvement in $g(z_0)$ over Eq. (24) and furthermore predicted a divergence in $w(z)$ at $z=L$. Presumably, these deficiencies would be rectified by the higher-order corrections, but their inclusion would be far too complicated to consider.

The principle effect of fluctuations is to transform the segment distributions $\rho(z;z_0,s)$ from the δ functions of Eq. (20) into broad Gaussian-like distributions similar to those of Eq. (38). This spread in the segment distribution produces an excess concentration near the substrate ($z\approx 0$) and the outer edge of the brush ($z\approx L$). The proximal-layer correction of Likhtman and Semenov[12] treats the former problem, and clears up several pronounced differences between SCFT and FCT. Perhaps the most significant is the δ function in $w(z)$ at $z=0$, which FCT fails to predict. The additional refinements to the field $w(z)$, the stretching energy $f_{0,e}(z_0)$, and the segment profiles $\phi(z;z_0)$ are equally impressive as demonstrated by Figs. 9, 10, and 11, respectively. No doubt, the present treatment of the proximal layer is sound.

The excess concentration at the outer edge, estimated in Fig. 12, requires a similar correction. To remove this excess, the peak of $g(z_0)$ must be shifted towards the substrate, which is precisely the type of correction needed to account for $\Delta g(z_0)$ in Fig. 4(b). Presumably, this would, in turn, correct the remaining inaccuracies in f_g and f_e [see Eqs. (36) and (37), and Fig. 7]. The only apparent hitch is that the corresponding correction to $w(z)$ required to shift the peak in $g(z)$ appears inconsistent with the $\Delta w(z)$ plotted in Fig. 2(b). Any reduction in segment concentration near $z\approx L$ should correspond to an increase in $w(z)$. However, we must remember that, in FCT, the sNth segment only interacts with $w(z)$ at a single point, $z=z_\alpha(s)$, whereas, in SCFT, it interacts with the field over the finite distribution $\rho(z;z_0,s)$. This distinction is most important when the curvature in $w(z)$ is large, as it is at $z=L$. Thus, it seems entirely reasonable that correcting $g(z_0)$ so as to fix the excess segment concentration in Fig. 12 and requiring the segments to interact with $w(z)$ over the finite distribution $\rho(z;z_0,s)$ would remove the last of the significant inaccuracies in the FCT.

Likhtman and Semenov[12] do adjust $g(z_0)$ so as to remove the excess segment concentration at $z\approx L$, but they do this assuming $\rho(z;z_0,s)$ is give by Eq. (29), which was obtained for the parabolic potential. This is their source of inaccuracy in the calculation of K_ξ. However, it is very likely that the accuracy could be greatly improved by simply using the estimate of $\rho(z;z_0,s)$ given by Eq. (38).

Not only can SCFT be used to verify strong-stretching corrections to SST, it can also identify mistaken proposals. Here, we call into question past SST-based calculations,[7,24] which assume the free energy of the brush is given by

$$\frac{f}{k_BT}=\frac{3\pi^2}{8a^2NL}\int z^2\phi(z)dz+\frac{a^2N}{24L}\int\frac{[\phi'(z)]^2}{\phi(z)}dz, \tag{41}$$

to within an additive constant. The first integral is a standard expression for the stretching energy,[3] and the second integral is a well-known penalty for a sharp change in the polymer concentration.[25] However, evaluating this expression for the predicted scaling profile in Fig. 6(b) gives the result,

$$\frac{f}{k_BT}=\frac{3\pi^2L^2}{8a^2N}+0.41\left(\frac{L}{aN^{1/2}}\right)^{-2/3}+\text{const}, \tag{42}$$

which seriously contradicts our fit in Eq. (40). Not only is the logarithmic term missing, the coefficient of 0.41 has the wrong sign. The validity of the first integral in Eq. (41) is reasonably certain, and so it is presumably the second integral that causes the problem. We suggest that the profile never meets the necessary requirement of sharpness.

Finite-stretching corrections are far more than an academic curiosity and are, in fact, critical in the calculation of certain quantities such as the positive tension $\gamma_{b/h}$ between a brush and its parent homopolymer responsible for the phenomena of autophobic dewetting.[7,8] The tension involves the difference between the free energy of a dry brush (as considered in this paper) and that of a brush in contact with homopolymer. Because the bare SST prediction for f cancels out, $\gamma_{b/h}$ is determined entirely by the finite stretching corrections. The fact that Ref. 7 treats these corrections using Eq. (41) implies that their results cannot be trusted. This conclusion also extends to SST-based calculations for the interaction between brushes as pertaining to, for example, colloidal stabilization,[26] because the physics is essentially the same.[8]

Unfortunately, we are unable to offer a similar explanation for the apparent discrepancy between the SCFT and SST predictions for the phase boundaries between the lamellar, cylindrical, and spherical morphologies of strongly-segregated A/B diblock copolymer melts.[10] In this case, the asymptotic limit for the boundaries is controlled by the dominant term in the free energy expansion [i.e., the first term in Eq. (1)], and its dependence on the curvature of the brush. That may, in fact, be where the problem lies. Our conclusion that SCFT properly converges to the present formulation of SST does not necessarily extend beyond flat interfaces. In a planar geometry, the lateral trajectory of the chain [i.e., $x_\alpha(s)$ and $y_\alpha(s)$] is decoupled from the stretching in the z direction,[8] but this is no longer true for curved brushes. Perhaps there are some subtleties with curved geometries that we are still unaware of. It would be worth exploring this possibility as the implications could extend far beyond the phase boundaries of block copolymer melts.

V. CONCLUSIONS

Detailed and accurate SCFT calculations were performed on thick (i.e., $2aN^{1/2}\leqslant L\leqslant 8aN^{1/2}$) polymeric brushes in order to investigate and test finite-stretching corrections to the conventional SST. This comparison has enhanced our general understanding of strongly stretched brushes in several ways. To start, it provided compelling evidence that SST is the correct asymptotic limit of SCFT, at least for flat brushes. However, it also demonstrated that extreme thicknesses are required before SST becomes accurate, implying that finite-stretching corrections are of considerable significance. Our study also differentiated between the effectiveness of competing strategies for incorporating such corrections, and identified one questionable treatment [i.e., Eq. (41)] used in several previous occasions.

We ultimately conclude that three distinct corrections are needed to bring SST into good agreement with SCFT. In practical terms, the most relevant correction comes from the entropy of the chain ends as treated by the FCT. This gives an average free energy per chain f that is well approximated by Eq. (35). The next two corrections involve fluctuations in the chain trajectory $z_\alpha(s)$ about the classical path of lowest energy. The fluctuations broaden the individual segment distributions, $\rho(z;z_0,s)$, causing an accumulation of segments near the substrate and the outer edge of the brush. A proximal layer extending $\mu=a^2N/6L$ from the substrate corrects for the first effect, increasing the stretching energy, particularly, of the weakly-stretched chains. On the other hand, the excess of segments near the brush edge requires a relaxation of the strongly-stretched chains. Although the Likhtman-Semenov theory does not provide an accurate treatment for this latter effect, their free energy expression in Eq. (1) remains accurate provided that we set $K_\xi=0.64$.

SST will undoubtedly remain a valuable theoretical tool because of its transparency and analytical predictions, and thus it is important to understand its leading corrections. The corrections are particularly significant for phenomena involving small excess free energies, such as interfacial tension and the interaction between brushes. In these instances, an incorrect treatment can actually invalidate the qualitative predictions of a SST-based calculation. Given the seriousness of this, it is certainly worth considering further tests against SCFT to validate other fundamental assumptions of the SST.

ACKNOWLEDGMENT

We are grateful to Sasha Semenov for valuable discussions and to Alexei Likhtman for providing details of their calculation in Ref. 12.

[1] A. N. Semenov, Zh. Eksp. Teor. Fiz. **88**, 1242 (1985) [Sov. Phys. JETP **61**, 733 (1985)].
[2] S. T. Milner, T. A. Witten, and M. E. Cates, Macromolecules **21**, 2610 (1988).
[3] M. W. Matsen, J. Phys.: Condens. Matter **14**, R21 (2002).
[4] S. F. Edwards, Proc. Phys. Soc. London **85**, 613 (1965); M. Doi and S. F. Edwards, *The Theory of Polymer Dynamics* (Clarendon, Oxford, 1986).
[5] E. Helfand, J. Chem. Phys. **62**, 999 (1975).
[6] M. W. Matsen and F. S. Bates, Macromolecules **29**, 1091 (1996).
[7] L. Leibler, A. Ajdari, A. Mourran, G. Coulon, and D. Chatenay, *OUMS Conference on Ordering in Macromolecular Systems*, edited by A. Tera-

moto, M. Kobayashi, and T. Norisuje (Springer, Berlin, 1994), pp. 301–311.
[8] M. W. Matsen and J. M. Gardiner, J. Chem. Phys. **115**, 2794 (2001); Note that the SST for $\gamma_{b/h}$ in the appendix contains a small error, where the 64 in Eq. (A3) should be replaced by 128 and the 16 in Eq. (A5) should be 32.
[9] G. Reiter and R. Khanna, Phys. Rev. Lett. **85**, 5599 (2000).
[10] M. W. Matsen and M. D. Whitmore, J. Chem. Phys. **105**, 9698 (1996); M. W. Matsen, *ibid.* **114**, 10528 (2001).
[11] J. L. Goveas, S. T. Milner, and W. B. Russel, Macromolecules **30**, 5541 (1997).
[12] A. E. Likhtman and A. N. Semenov, Europhys. Lett. **51**, 307 (2000).
[13] T. A. Witten, L. Leibler, and P. A. Pincus, Macromolecules **23**, 824 (1990).
[14] M. W. Matsen and F. S. Bates, Macromolecules **28**, 8884 (1995).
[15] R. R. Netz and M. Schick, Europhys. Lett. **38**, 37 (1997); Macromolecules **31**, 5105 (1998).
[16] M. W. Matsen, J. Chem. Phys. **117**, 2351 (2002).
[17] M. W. Matsen and J. M. Gardiner, J. Chem. Phys. **118**, 3775 (2003).
[18] Without a field to enforce a uniform concentration of grafted polymers, the distribution of end segments goes as $g(z_0)\propto\exp(-3z_0^2/2a^2N)$, which would imply an average chain extension of $\langle z_0\rangle=(2a^2N/3\pi)^{1/2}=0.46aN^{1/2}$.
[19] S. T. Milner, Science **251**, 905 (1991).
[20] S. T. Milner, J. Chem. Soc., Faraday Trans. **86**, 1349 (1990).
[21] K. Ø. Rasmussen and G. Klosakas, J. Polym. Sci., Part B: Polym. Phys. **40**, 1777 (2002).
[22] R. L. Burden, J. D. Faires, and A. C. Reynolds, *Numerical Analysis*, 2nd ed. (PWS, Boston, 1981).
[23] A. N. Semenov (private communication).
[24] A. N. Semenov, Macromolecules **25**, 4967 (1992); **26**, 2273 (1993).
[25] D. Broseta, G. H. Fredrickson, E. Helfand, and L. Leibler, Macromolecules **23**, 132 (1990); P.-G. de Gennes, *Scaling Concepts in Polymer Physics* (Cornell University Press, Ithaca, 1979), p. 254.
[26] I. Borukhov and L. Leibler, Phys. Rev. B **62**, R41 (2000).